Silicon Carbide UV Photodiodes

Dale M. Brown, *Fellow, IEEE*, Evan T. Downey, Mario Ghezzo, *Member, IEEE*, James W. Kretchmer, Richard J. Saia, Yung S. Liu, *Member, IEEE*, John A. Edmond, George Gati, Joseph M. Pimbley, *Senior Member, IEEE*, and William E. Schneider

Abstract—**SiC photodiodes were fabricated using 6H single-crystal wafers. These devices have excellent UV responsivity characteristics and very low dark current even at elevated temperatures. The reproducibility is excellent and the characteristics agree with theoretical calculations for different device designs. The advantages of these diodes is that they will operate at high temperatures and are responsive between 200 and 400 nm and not responsive to longer wavelengths because of the wide 3-eV bandgap. The responsivity at 270 nm is between 150 and 175 mA/W with a quantum efficiencies of between 70% and 85%. Dark-current levels have been measured as a function of temperature that are orders of magnitude below those previously reported. Thus these diodes can be expected to have excellent performance characteristics for detection of low light level UV even at elevated temperatures.**

I. Introduction

AN ADVANTAGE of SiC photodiodes is that because of the wide bandgap of 6H SiC (3 eV) there is no responsivity to IR radiation which is important for certain applications whenever it is desirable to detect UV in an IR background. Another advantage is that SiC devices could be utilized in a high-temperature environment because the wider bandgap should lead to a very low level of diode dark current. This is especially important when low-level photon fluxes need to be detected.

Previous efforts at making SiC photodiodes have utilized N-ion implantation to form a very shallow n^+ junction in a p-type 6H SiC epitaxial layer and by Al diffusion into 6H n-type crystals [1], [2].

The N-ion implantation method utilized a very low energy implantation to form a very shallow (0.05-μm) junction in order to enhance the short-wavelength response. However, contact sintering at high temperatures could induce diffusion of the contact metal through crystalline defects in this thin layer and thereby increase diode leakage. The method of making the p^+-n photodiodes using Al diffusion required very high temperatures (2180°C) and long times (20 h) [3].

Manuscript received August 2, 1992. The generation of data in Fig. 10 was supported by The Air Force under Contract F33615-90-C-2011. The review of this paper was arranged by Associate Editor J. J. Coleman.

D. M. Brown, E. T. Downey, M. Ghezzo, J. W. Kretchmer, R. J. Saia, and Y. S. Liu are with General Electric Corporate Research and Development, Schenectady, NY 12301.

J. A. Edmond is with Cree Research Inc., Durham, NC 22713.

G. Gati is with GE Aircraft Engines, Cincinnati, OH 45249.

J. M. Pimbley is with Rensselaer Polytechnic Institute, Troy, NY 12181.

W. E. Schneider is with Optronic Laboratories, Inc., Orlando, FL 32811.

IEEE Log Number 9205318.

This paper describes results of photodiodes made using n- and p-type epitaxial layers. This approach for making SiC photodiodes avoids the difficulties of the two methods previously utilized. Optical and electrical characteristics are given as a function of temperature to 400°C. An optical model is derived and compared with experimental results. Optical responsivity data are compared with analytical quantum efficiency calculations.

II. Device Fabrication

Single-crystal 6H SiC wafers, 1 inch in diameter, were used as substrates. Devices were made using either n- or p-type doped substrates. Al-doped p-type epitaxial layers 1 to 5 μm thick were grown on these substrates. A heavily N-doped n-type epitaxial layer of 0.2 or 0.3 μm thick was utilized to form an n^+-p junction. Wafers of this type are available from Cree Research. The concentrations of impurities in each epitaxial layer is given in Table I. The device mesa was patterned and etched using RIE and an NF_2/O_2 gas mixture. Different mesa dimensions were utilized these being 1×1 mm^2, 2×2 mm^2, 3×3 mm^2. For some devices, the n^+ area outside of the n^+ contact region on the top of the mesa was thinned by RIE to thicknesses less than 0.1 μm to increase the short-wavelength response. This avoids yield losses caused by the contact sintering step. The device cross section is shown in Fig. 1. Device passivation was accompanied by growing a thin (0.05-μm) layer of SiO_2 and in some cases adding a chemical vapor deposited layer of SiO_2 using SiH_4 and O_2 over the top of this thermally grown layer for a total thickness of 0.6 μm (see Table I). When n-type substrates were used, a top contact (Al) was made to a p^+ layer initially grown on the n-type substrates before growing a more lightly doped p layer. This was done to reduce the diode's series impedance. The contact to the top n^+ layer was Ni. This contact comprising a simple cross in the middle of the mesa covered less than 2% of the mesa's area. Contact sintering was done in Ar at temperatures between 900 and 1000°C.

III. Device Measurement Methods

Diode electrical characteristics were measured as a function of temperature using Hewlett-Packard and Keithly electrometers. Optical responsivity measurements were made using the double monochrometer shown in Fig. 2. This system was optimized for measurements over the 200 to 450-nm wavelength region.

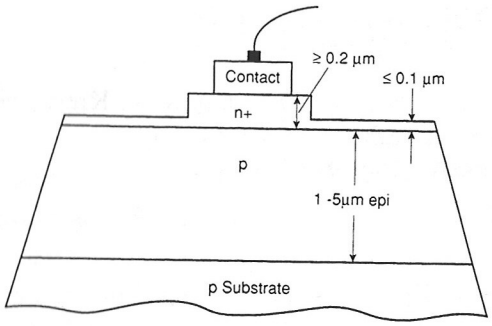

Fig. 1. Photodiode device structure.

TABLE I
DEVICE STRUCTURES

Device	Substrate	p-Layer Epi	n^+-Layer Thickness	SiO_2 Passivation
1, 2	p	1 μm p^+, 1 μm p	0.2 μm	0.05 μm
3, 4	p	1 μm p^+, 1 μm p	0.3 μm	0.05 μm
5	n	1 μm p^+, 1 μm p	0.075 μm	0.6 μm
6	p	5 μm p	0.05 μm	0.055 μm

Dopant Layer Concentrations		
p substrate	Al	5 to 8 × $10^{17}/cm^3$
n substrate	N	0.5 to 1 × $10^{18}/cm^3$
p^+ layer	Al	2 to 3 × $10^{18}/cm^3$
p layer	Al	1.2 to 3 × $10^{17}/cm^3$
n^+ layer	N	5 to 10 × $10^{18}/cm^3$

A system employing a double monochromator for the optical dispersing mechanism was considered essential in order to minimize the effect of stray light. Outstanding attributes of the monochromator are its fast optical speed ($f/4$), grating efficiencies at blaze wavelengths of greater than 70%, and an extremely low scattered light level. Gratings blazed at 250 nm were selected in order to optimize the monochromator performance over the 200–450-nm wavelength region. Specifications for the double monochromator are given below.

wavelength range (W/300-nm gratings)	200 to 500 nm
dispersion	2 nm/mm
wavelength accuracy	±0.2 nm
wavelength precision	±0.1 nm
bandwidth	0.5, 1, 2.5, 5, and 10 nm
stray light	less than 10^{-6}

A filter wheel controller was used to control the wavelength and the second-order blocking filters. The light source consisted of a 150-W quartz halogen lamp and a 50-W deuterium lamp. The sources can be imaged onto the entrance slit of the double monochromator through the use of a manual beam switching mirror. A quartz lens collimator was attached to the exit port of the double monochromator. This attachment uses a 7.6-cm focal length fused silica lens to semi-collimate the monochromatic beam exiting the monochromator. A 6-mm-diameter aperture was placed at the end of the collimating tube. This provided a well-defined, uniform beam for irradiating both the standard detector and the SiC photodiode with the same monochromatic flux. The detector used for calibration consisted of an enhanced silicon detector which was attached directly to the end of the collimating tube. An autoranging radiometer/photometer was used to measure the current generated by the detector. This instrument has full scale ranges from 10^{-4}–10^{-10} A and a resolution of 10^{-13} A. Both wavelength and detector signals were transmitted to a PC and enabled the PC to control the entire measurement process and data reduction on a real-time basis. The pertinent optical parameters for the measurements were as follows:

wavelength range	200 to 450 nm
half bandwidth	5 nm

Calibration of the UV-enhanced silicon detector is based on calibrations performed by the Far UV Physics Group below 250 nm at NIST (National Institute of Standards and Technology) [4]. The uncertainty in the reported spectral response values is ±5%. For the region above 250 nm, the calibration is based on the NIST Photodetector Spectral Response Calibration Transfer Package [5]. The reported uncertainty in the NIST scale over the wavelength range of 250 to 450 nm varies from ±6% to ±4%. The transfer uncertainty to the calibrated detector is estimated at ±1%. Accordingly, the uncertainty in the monochromatic flux at the end of the quartz lens collimator relative to the NIST scale is estimated to be less than ±2% over the 200- to 450-nm wavelength range. The precision or ability to repeat measurements on the SiC photodiodes was on the order of ±5%. The final uncertainty in the measurements is a combination of the uncertainty in the monochromatic flux and repeatability uncertainty.

The optical system was calibrated by scanning wavelength and measuring the response of the calibrated Si reference diode. The SiC photodiode responsivity was then determined by replacing the Si reference diode with a SiC photodiode unit and repeating the wavelength scan. This unit consisted of an Au plated kovar multiple pin package header upon which a SiC photodiode chip or die had been die- and wire-bonded. The short-circuit photocurrent was measured to obtain the responsivity in milliamperes per watt, and the quantum efficiency was determined from these responsivity numbers using the simple formula

$$\text{Q.E.} = 1.241 \times \frac{\text{responsivity (mA/W)}}{\text{wavelength (nm)}}. \quad (1)$$

This is the so-called "external" quantum efficiency since the responsivity of the device was measured without correcting for reflection and therefore, represents the current generated for a watt of photon flux incident on the device.

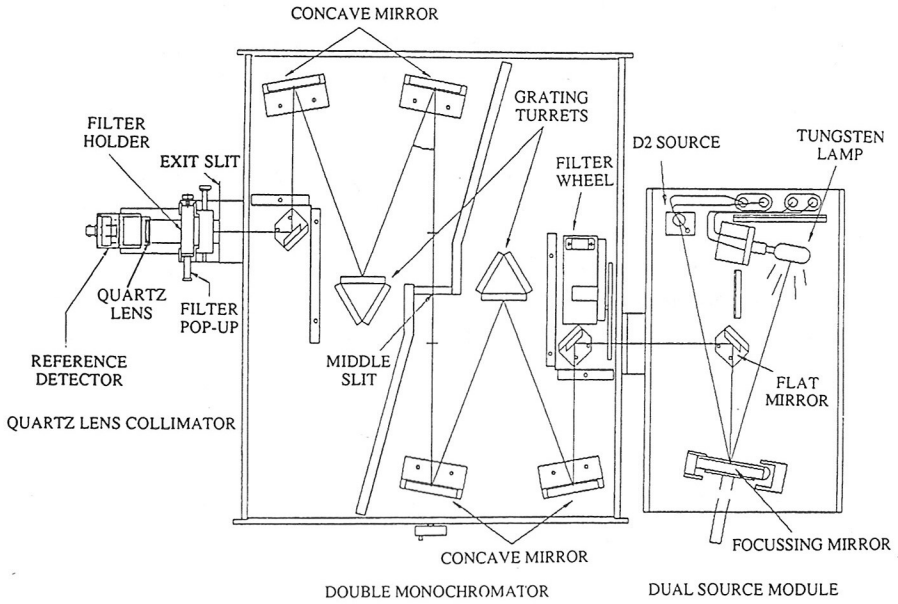

Fig. 2. Optical schematic of the double monochrometer utilized to make photoresponsibility measurements.

IV. SiC Photodiode Quantum Efficiency Model

In order to model the external quantum efficiency, the transmission of light through the oxide passivation layer and the generation and collection of carriers at the junction must be considered. Incident radiation traverses a layer of SiO_2 before entering the shallow n^+ region. Various fractions of the transmitted radiation are absorbed within this surface n^+ layer, then p epilayer, and the substrate. We presume that each absorbed photon generates one hole–electron pair within the silicon carbide. The quantum efficiency, then, is the number of electrons detected divided by the number of incident photons. The model has three primary components: transmission of light through any and all overlying films and into the silicon carbide, absorption within the various regions of the silicon carbide, and collection of the charge generated by photon absorption at the n^+-p junction. A previous modeling study neglected the first component and simplified the third component [2].

We compute transmission of light through an arbitrary number of films by solving Maxwell's equation for plane waves at normal incidence [6]. This optical modeling capability is essential since films overlying the substrate can alter the total quantum efficiency via interference phenomena and absorption. Once radiation enters the silicon carbide, one finds a simple exponential attenuation. Thus absorption within the surface n^+ region, p epilayer, and substrate are easily extracted. For these portions of the model it is essential to include accurate wavelength-dependent optical data. We utilized the results of Philipp and Taft [7]; however, the tabulation of SiC optical data published by Choyke and Palik could also have been used [8].

Finally, we describe the charge collection portion of the model. A previous study by Glasow *et al.* [1] emphasized the importance of both surface and bulk recombination. Thus we assign a surface recombination velocity s to the SiC–SiO_2 interface at $x = 0$ as well as a bulk diffusion length to each of the epitaxial layers. A hole generated within the n^+ layer may recombine at the surface, recombine within the bulk, or contribute to the detected signal by diffusing to the n^+-p junction. Similarly, an electron generated within the p region may be lost to the substrate and recombine within the bulk or add to the detected signal by diffusing to the n^+-p junction. Thus the desired total quantum efficiency consists of a hole component (for photons absorbed within the n^+ layer) and an electron component (for photons absorbed within the p region). This charge collection portion is essentially the internal quantum efficiency or the efficiency after the photon has entered the silicon carbide and when coupled with the light transmission calculation which includes the oxide layer on the surface, the model gives the external quantum efficiency or the efficiency of collected photogenerated carriers for radiation incident on the structure. The optical constants utilized for the SiO_2 passivation layer were obtained from [9].

For the hole component, we write a steady-state, one-dimensional diffusion equation with diffusion length L_p as[1]

$$\frac{d^2p}{dx^2} - \frac{p}{L_p^2} = -A(x) \tag{2}$$

where $A(x)$ is proportional to the density of absorbed energy at depth x in the silicon carbide. The diffusion length L_p in (2) is defined as the square root of the product of

[1]The notation is regrettably prone to misinterpretation. The subscript p in L_p denotes its definition as a hole diffusion length. But the reader must bear in mind that this hole diffusion length is a property of the n^+ layer only. Within the p layer, for example, we would write the electron diffusion length as L_n.

hole diffusivity and recombination lifetime. The Dirichlet boundary condition $p(X_n) = 0$ is appropriate for modeling collection of holes at the n^+-p junction while the condition $D_p p'(0) - sp(0) = 0$ at the SiC–SiO_2 interface at $x = 0$ specifies the recombination of carriers at the interface with surface recombination velocity s. Noting that (2) generation term $-A(x)$ is proportional to the exponential attenuation $\exp(-\alpha x)$, we solve (2) and the associated boundary conditions for $p(x)$. We then compute the quantum efficiency component η_p for photons absorbed within the n^+ layer by deriving the current reaching the n^+-p junction. We find

$$\eta_p = \frac{\alpha L_p}{\alpha^2 L_p^2 - 1}\left\{\frac{\alpha D_p + s - \left[\frac{D_p}{L_p}\sinh\frac{X_n}{L_p} + s\cosh\frac{X_n}{L_p}\right]e^{-\alpha X_n}}{\frac{D_p}{L_p}\cosh\frac{X_n}{L_p} + s\sinh\frac{X_n}{L_p}} - \alpha L_p e^{-\alpha X_n}\right\}. \tag{3}$$

For those samples that utilized a p^+ layer to reduce the series resistance to the top contact to this layer, the component η_n for photons absorbed within the p/p^+ region is treated similarly. Both boundary conditions (at $x = X_n$ and $x = X_n + X_p$) are of the vanishing Dirichlet type. But for devices with p and p^+ layers, we allow the diffusion lengths to differ in the two layers. We require the current density to be continuous at this interface (which here implies continuity of $n'(x)$) and we note that the electron concentration will suffer a jump discontinuity due to the built-in potential difference between the p and p^+ layers. We therefore infer the appropriate jump condition from the acceptor concentrations of the p and p^+ layers. Again we solve the electron diffusion equation in light of the boundary and interface conditions and compute the electron current at the n^+-p junction to get the electron contribution to the total quantum efficiency as

$$\eta_n = \frac{\alpha L_n e^{-\alpha X_n}}{\alpha^2 L_n^2 - 1}\left\{\alpha L_n - \tanh\frac{X_p}{L_n} - \frac{\alpha L_n e^{-\alpha X_p}}{\cosh\frac{X_p}{L_n}}\right\}$$

$$+ \frac{\alpha L e^{-\alpha(X_n + X_p)}}{(\alpha^2 L^2 - 1)\cosh\frac{X_p}{L}}$$

$$\cdot\left\{\alpha L + \frac{e^{-\alpha X_{p+}} + \cosh\frac{X_{p+}}{L}}{\sinh\frac{X_{p+}}{L}}\right\}. \tag{4}$$

In equation (4), L_n is the diffusion length of electrons in the p region while L stands for the diffusion length of electrons in the p^+ layer. We have also simplified (4) because the difference in acceptor concentrations of the p and p^+ layers is "large" (i.e., at least a factor of ten). The analytical quantum efficiency calculations varied the diffusion length of holes in the n^+ layer and electrons in the p layer to fit the experimental data.

This model does not include the effect of a depletion region at the n^+-p junction. The extent of this region is very small ($\sim 0.15\ \mu m$) because of the heavy dopant concentration in the p layer ($10^{17}/cm^2$) and is much smaller than the p-layer thicknesses utilized in this study. Therefore, inclusion of the depletion layer would not contribute significantly to the quantum efficiency.

V. Experimental Results and Discussion

A. Reverse Bias Leakage

The reverse bias leakage current at 10 V bias as a function of temperature is plotted in Fig. 3 and compared to previously published results obtained from n^+-p diodes formed utilizing N-ion implantation on 6H SiC [1].

The leakage levels of the epitaxial diodes are very low being two to four orders of magnitude less than the leakage of the ion-implanted diodes. The epitaxial diode reverse bias leakage is also many orders of magnitude less than typical silicon diodes whose dark current levels are typically between 0.5 and 1 nA/cm^2 at 25°C but as high as 10 mA/cm^2 at 300°C and 10 A/cm^2 at 500°C. In contrast, the diode leakage of 2 × 2 mm SiC photodiodes at 300°C is as low as about 10 nA/cm^2. This is six orders of magnitude less than a typical Si diode.

The low leakage level of the mesa-type epitaxial diodes produces much larger photovoltages for low light level applications. This is because the open circuit photovoltage is determined by the diode's forward characteristic and the short circuit photocurrent which is dependent upon the quantum efficiency or optical responsivity. Low dark current levels also increase the dynamic range and reduce shot noise. All these factors are important whenever it is required to detect low level UV signals in a high-temperature environment.

B. Optical Responsivity

The optical responsivity and quantum efficiency as determined by measuring the short-circuit current were determined for a number of devices made using different epitaxial layer thicknesses. These variations are shown in Table I.

Fig. 4 plots the responsivity for devices 1, 2, 3, and 4. Notice that the short-wavelength responsivity increases

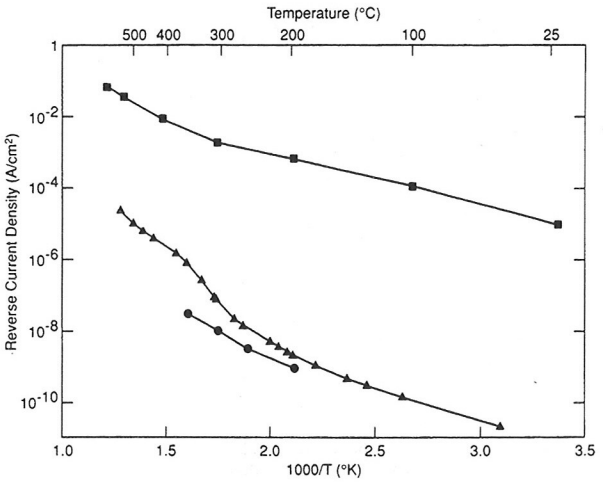

Fig. 3. Normalized (A/cm^2) reverse current leakage at 10 V versus $1000/T$ (K) of photodiodes that utilized N-ion implantation to form the n^+-p junction (1) given by the upper curve (square data points); all epitaxial layer diodes, high-voltage diode $A = 3.7 \times 10^{-3}$ cm^2 (triangular points) and photodiode, $A = 4 \times 10^{-2}$ cm^2 (circular points).

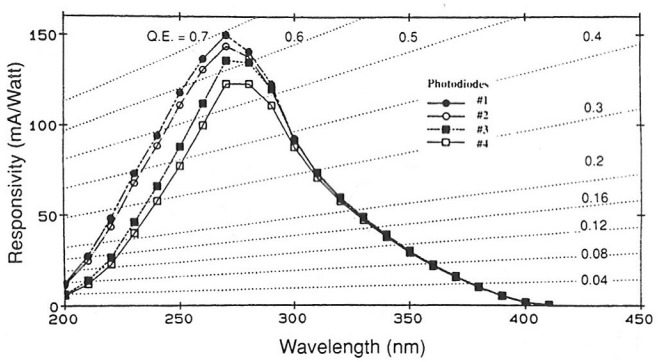

Fig. 4. Spectral responsivity curves of diodes #1, 2 with 0.2-μm n^+ epi and diodes #3, 4 with 0.3-μm n^+ epi. Notice a reduction of short-wavelength response with thicker n^+ epi.

when the n^+ epitaxial layer thickness is decreased from 0.3 to 0.2 μm because the optical absorbance is very high for short wavelengths and the surface recombination velocity is also high. In fact, to model the experimental measurements, we found it necessary to make the surface recombination velocity infinite. Because the surface recombination velocity is high, the implication is that the surface of the SiC which has been passivated with a thermally grown SiO_2 layer contains large numbers of recombination centers. For instance, it is likely that the surface of the p-type SiC on the sidewalls of the mesa contains a large number of SiO_2/SiC fast interface states that act as surface recombination centers. The long-wavelength response, as shown, is unaffected by the upper layer thickness because the optical absorbance is decreasing rapidly with wavelength as the incident photon energy approaches that of the bandgap.

In order to increase the longer wavelength photoresponse and to determine the diffusion length of electrons, thicker 5-μm epitaxial p layers were utilized (device 6). In addition, in order to increase the short-wavelength response, devices 5 and 6 used thinner n^+ layers. The measured responsivity curves for devices 5 and 6 are shown in Figs. 5 and 6. The data for devices 5 and 6 are replotted as quantum efficiency and compared with analytical calculations in Figs. 7 and 8. The responsivity curve for device 5 shows the influence of optical interference effects produced by the thicker SiO_2 passivation layer employed (see Table I).

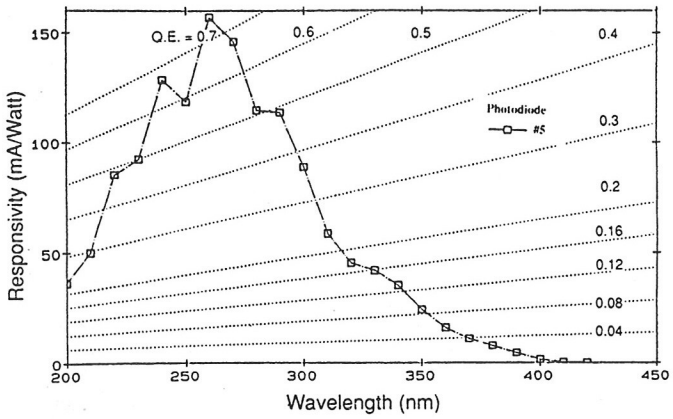

Fig. 5. Spectral responsivity curve of diode #5 with 0.075-μm n^+ epi to enhance short-wavelength response. The curve jagged shape is caused by thicker SiO_2 passivation (0.6 μm).

C. Photocurrent Produced by 257-nm Argon Laser Light

Diode short-circuit output current was also measured at 257 nm as a function of optical input power using an argon ion laser and a frequency-doubling crystal (Fig. 9). This diode with an area of 2×2 mm^2 was constructed like samples 1 and 2 and the output current agrees well with the responsivity measurements of Fig. 4.

D. Responsivity as a Function of Temperature

The responsivity of the photodiode at higher temperatures will shift to longer wavelengths because of bandgap narrowing; however, the UV responsivity should continue to be excellent to temperatures as high as 400°C as shown by Glasow *et al.* [1]. Fig. 10 verifies this and shows that the responsivity increases on the long-wavelength side of the responsivity curve because the bandgap decreases and hence absorption increases as the temperature increases. However, one distinct difference is noticeable. The peak response in Fig. 10 increases as the temperature increases whereas in [1], the peak response decreased.

E. Electron Diffusion Length

Glasow *et al.* suggested that the diffusion length of electrons must be greater than 1 μm [1]. Their argument was based on a lifetime of 20 ns for electrons and holes

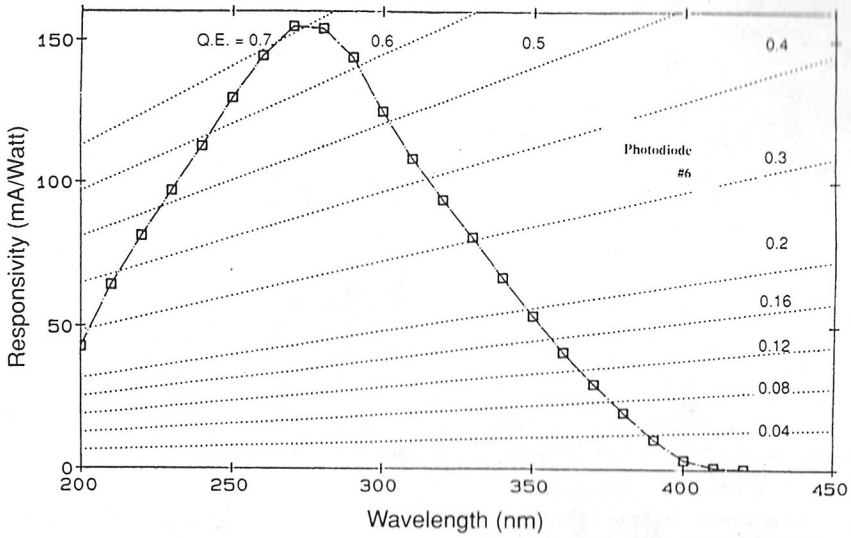

Fig. 6. Spectral responsivity curve of diode #6 with 0.050-μm n^+ epi over 5-μm p epi. The long-wavelength responsivity is increased by the thicker p epilayer.

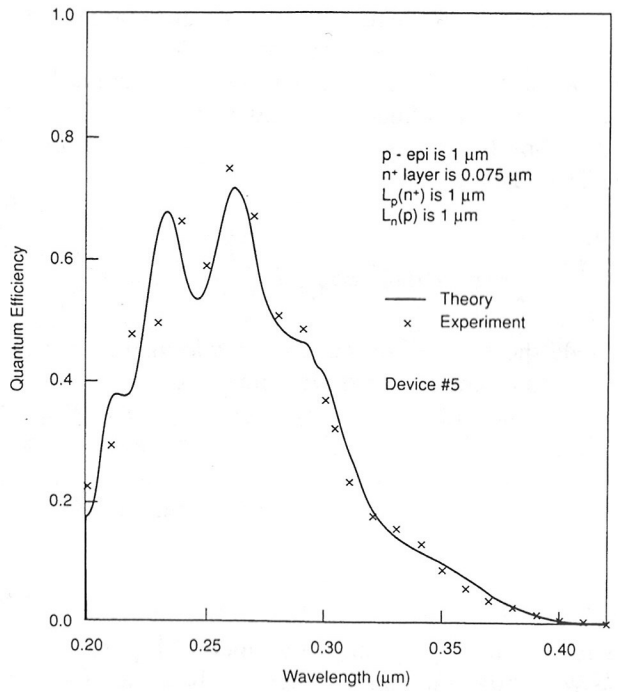

Fig. 7. Quantum efficiency versus wavelength for device #5 comparing experimental modeling results.

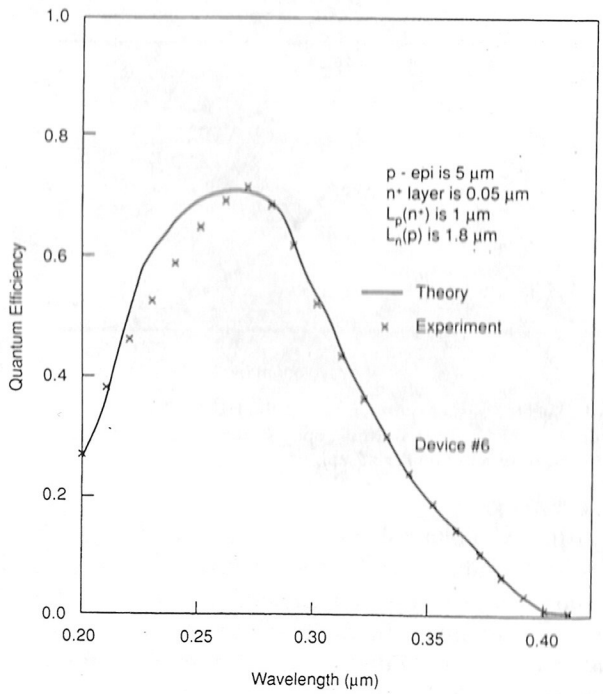

Fig. 8. Quantum efficiency versus wavelength for device #6 comparing experimental and modeling results.

and an electron mobility of 200 $cm^2/V \cdot s$ which gives a diffusion length of 3 μm for electrons.

For the quantum efficiency calculations for device 6 (Fig. 8) the diffusion length of electrons in the p layer was varied and it was found that the sensitivity of the fit to the electron diffusion length was quite high. The diffusion length of 1.8 $\pm$ 0.4 μm is smaller than the estimate of 3 μm given in [1]. This diffusion length determination does not depend on any assumptions about carrier lifetime and mobility. Diffusion length is an important device parameter for bipolar transistor design for example.

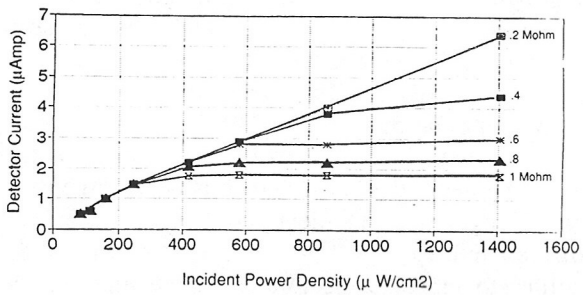

Fig. 9. Detector photoresponse curves at λ = 257 nm for various resistor loads using an argon-ion laser source and a frequency-doubling crystal. Area is 2 $\times$ 2 mm^2.

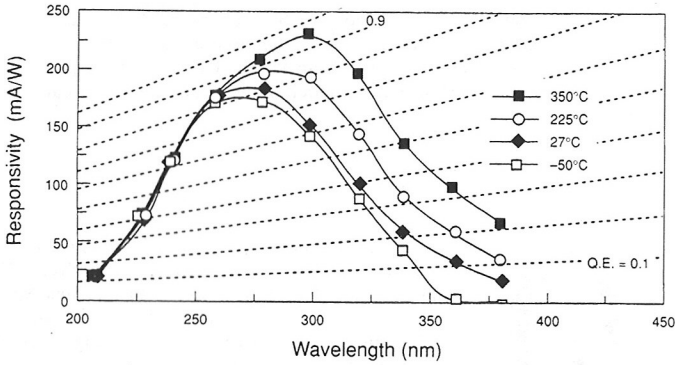

Fig. 10. Responsivity versus wavelength for different temperatures: −50°C, 27°C, 225°C, and 350°C.

VI. Summary

SiC photodiodes made using 6H epitaxial layers on 6H substrates were fabricated and tested. The electrical and optical characteristics to temperatures as high as 350°C were determined. Optical responsivity with a peak at about 270 nm of between 150 and 175 mA/W with a quantum efficiency of about 70% to 85% was measured. Thinning of the top n^+ layer outside of the mesa contact proved to be a good method of enhancing the short-wavelength response and diodes made using very thin n^+ layers had responsivities as high as about 50 mA/W at 200 nm. The responsivities reported here are similar to these reported in [1]. The reverse-bias diode leakage, however, was shown to be much lower than that reported in [1].

The characteristics of these diodes were predictable using an optical responsivity or quantum efficiency model based on published 6H SiC optical absorbance data and reasonable values of the electron and hole diffusion lengths. The electron diffusion length in 6H SiC was determined to be 1.8 ± 0.4 μm.

Acknowledgment

The authors wish to thank R. Guida for his help using gas laser light sources to measure photoresponse.

References

[1] P. Glasow, G. Ziegler, W. Suttrop, G. Pensl R. Heibeg, "SiC-UV-photodetectors," *SPIE*, vol. 868, pp. 40–45, 1987.

[2] R. B. Campbell and H. C. Chang, "Detection of ultraviolet radiation using silicon carbide p-n junctions," *Solid-State Electron.*, vol. 10, pp. 949–953, 1967.

[3] H. C. Chang, L. F. Wallace, and C. Z. LeMay, in *Proc. Conf. on SiC*. New York: Pergamon, 1960, p. 496.

[4] R. P. Madden, "UV and VUV radiometry at NIST," presented at the CORM '89 Int. Conf. on Optical Radiation Measurements, May 17–19, 1989.

[5] E. F. Zalewski, NBS Measurement Series: "The NBS Photodetector Spectral Response Calibration Transfer Program," NBS Special Publ. 250-17, Mar. 1988.

[6] J. M. Pimbley and G. J. Michon, "Charge detection modeling in a solid state image sensor," *IEEE Trans. Electron Devices*, vol. ED-34, no. 2, p. 294, 1987.

[7] H. R. Philipp and E. A. Taft, *Intrinsic Optical Absorption in Single Crystal Silicon Carbide*. Oxford, UK: Pergamon, 1960.
H. R. Phillipp, "Intrinsic optical absorption in single crystal silicon carbide," *Phys. Rev.*, vol. 111, p. 440, July 1958.

[8] W. C. Choyke and E. D. Palik, "Silicon carbide (SiC)," in *Handbook of Optical Constants of Solids*. New York: Academic, 1985, pp. 587–595.

[9] D. R. Lide, *Handbook of Chemistry and Physics*, 73 ed. Boca Raton, FL: CRC Press, 1992.

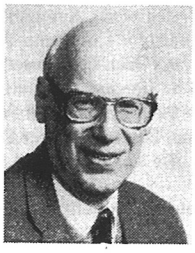

Dale M. Brown (SM'71–F'88) received the B.S. and M.S. degrees in physics from the University of Michigan, Ann Arbor, and Ph.D. degree, also in physics, from Purdue University, West Lafayette, IN.

At the General Electric Corporate Research and Development, Schenectady, NY, his research studies include GaAs devices, thermoelectric cooling, silicon–silicon dioxide interface states, MOSFET devices, silicon nitride passivation (MNOS), doped-glass diffusion sources and interlevel dielectrics, and refractory metal technology for use in IC's. He has also directed projects on solid-state relays using optoelectronic sensors, high-density CID imagers, and power MOSFET's. He directed the technical efforts to develop the GE VLSI VHSIC type 1.25- and 0.8-μm CMOS processes including multilevel metal and analog functions. Currently, he is working on SiC device research for advanced GE engine controls and doing research on novel devices for GE Medical Systems. He has written 77 papers in his field and has been awarded 38 patents. He is a GE Coolidge Fellow and is the recipient of the 1990 Electrochemical Society's Electronics Division Award.

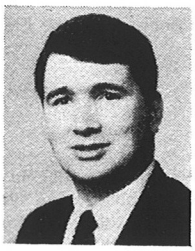

Evan T. Downey received the B.S. degree in applied software science from Rochester Institute of Technology, Rochester, NY, and the M.S. degree in computer science from Rensselaer Polytechnic Institute, Troy, NY.

He is a Supervising Parametric Test Engineer at General Electric's Research and Development Center, Schenectady, NY. His major professional interest is the development of automated test and data acquisition systems used to characterize IC processes. As a part of a research team responsible for the development of IC manufacturing processes, he has written software systems used to gather, store, reduce, and analyze parametric data.

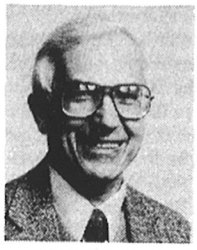

Mario Ghezzo (M'81) received the Ph.D. degree.

He is a Staff Physicist at General Electric Corporate Research and Development Center, Schenectady, NY. He has worked for over 20 years on MOS device technology, making numerous contributions in the fields of preparation and characterization of thin films, device design and fabrication, and technology development. He was part of the GE team which developed Charge Injection Devices for television cameras to replace vidicon tubes. He played a key role in the VLSI program at GE, leading in development of the 1.25-μm CMOS/BULK process, and later contributing to scaling this process to 0.8 μm. He was directly responsible for the process architecture, process flow and design rules, and participated in the process technology transfer to production. Currently, he is doing research on SiC device technology and multichip modules yield enhancement. He is author or co-author of 48 papers and holds 15 patents. He is also a co-author of volume 19 of Academic press VLSI Electronic Series, titled *Advanced CMOS Process Technology* edited by N. Einspruch. In the last four years he lectured at the Short Course on VLSI Yield Enhancement, held at Rensselaer Polytechnic Institute, Troy, NY.

James W. Kretchmer received the B.S. degree in photographic science from the Rochester Institute of Technology, Rochester, NY, in 1979.

Prior to joining General Electric Co. he held Microlithography positions including Supervising Process Engineer at Fairchild Semiconductors, South Portland, ME, and Senior Applications Engineer at Allied Chemical Electronic Chemical Division, Buffalo, NY. He joined General Electric Co. in 1986, and is currently Supervising Engineer responsible for silicon power device and silicon carbide device fabrication activities in the Electronic Assemblies and Device Fabrication Laboratory of General Electric's Corporate Research and Development Center, Schenectady, NY. As such he is responsible for on-line supervision of processing as well as process integration for these programs. Since joining G.E. he has also been involved in fabrication programs for Smart Power IC, miscellaneous Discrete Power Devices, and Amorphous Silicon Flat Panel Displays. He has co-authored 6 technical papers.

Mr. Kretchmer is a member of the Society of Photo Instrumentation Engineers.

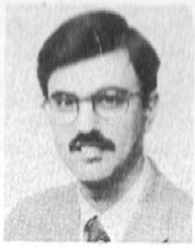

Richard J. Saia received the B.S. and M.S. degrees in physical chemistry from the University of Massachusetts, Boston.

He is currently the Supervising Engineer for plasma processing in the Electronic Technology Laboratory of General Electric's Corporate Research and Development Center, Schenectady, NY. He has been involved in the development of new plasma etching processes, CVD tungsten processes, and methods of fabricating advanced structures for VLSI, power, SiC, LCD, HDI, and micromechanical applications since 1981, when he joined the Center as a Chemist. During that time he has authored 30 technical papers, and holds 5 patents.

Mr. Saia is a member of the American Chemical Society and the Electrochemical Society.

Yung S. Liu (M'87) received the B.S. degree in physics from National Taiwan University in 1966 and the Ph.D. degree in applied physics from Cornell University, Ithaca, NY, in 1973.

He has been at General Electric's Research and Development Center, Schenectady, NY, since 1972, and is a Senior Scientist in the Electronic Technology Laboratory. His specialties are electrooptics, laser and nonlinear optics, and high-density interconnect technologies. He received a GE Outstanding Achievement Award in 1977 for his contribution to high-power solid-state laser and nonlinear optical technology. In 1981, he led a successful transition of the solid-state laser technology to GE business. From 1979 to 1982, under the USAF sponsorship, he and Dr. R. Belt of Litton led the research effort to develop the process for growing large nonlinear KTP crystal which has become one of the most commonly used nonlinear crystals. In 1982, he was the first one to develop the high-average-power intra-cavity frequency-doubled YAG laser. This type of laser device is now widely used for material processing, as well as electronic and medical applications. In 1986, he led the research effort in developing adoptive laser processing technologies for microelectronic interconnect applications, and is a principal investigator of a 5-year program, sponsored by the U.S. Office of Naval Research, developing advanced laser interconnect technologies for high-speed electronic systems. His current research activities include optical and high-density interconnects for advanced electronic packaging. In addition, he is an Adjunct Professor of Physics at the State University of New York at Albany, and is serving on the Advisory Committee on Lasers and Electrooptics Technology at the Hudson Valley Community College, Troy, NY. He is also serving on the proposal review panel for the New York State Sciences and Technology Foundation. He has authored and co-authored over 80 papers, and was granted 11 patents. He is the author of a book chapter n *Laser Microfabrication and Lithography* published by Academic Press in 1989.

Dr. Liu is a member of the American Physical Society, the Optical Society of America, the Materials Research Society, and the American Vacuum Society.

John A. Edmond received the B.S. degree in ceramic engineering from Alfred University, NY, and the Ph.D. degree from North Carolina State University, Raleigh, in materials science and engineering, with a minor in electrical engineering.

Since his graduation in September of 1987, he has been a senior scientist at Cree Research, Inc., Durham, NC, concentrating on the development of p-n junction diodes and blue LED's and device processing techniques. He is a cofounder of Cree Research, Inc. He has over 30 publications and 10 patents concerning semiconducting SiC.

George Gati received the B.S. and M.S. degrees in electrical engineering from the University of Cincinnati, Cincinnati, OH, in 1963 and 1965, respectively. He also completed additional post-graduate work in electrical engineering.

He joined GE Aircraft Engines, Cincinnati, in 1963. From 1963 to 1969, as an Electrical Systems Engineer for GE's Nuclear Systems Program, he designed turbogenerators, electromagnetic pumps, and a synchronous static frequency divider. From 1969 to 1984, he held the position of Electrical Circuit Design Engineer and was responsible for nuclear radiation hardening of engine electronic control systems for the B-1 bomber and the KC-135 tanker. As a Project Engineer, he was responsible for developing a large 4 × 4.5 in, 10-layer, cofired, hermetically sealed ceramic hybrid processor module and for establishing producibility and proof of reliability. He received a Managerial Award for his efforts in designing, building, and equipping a clean room facility for building thin-film strain gauges and hybrids, and for introducing the first in-house designed and built hybrid circuitry. In 1984, he assumed the position of Senior Engineer, Hybrid and Nuclear Technology, and was named Senior Engineer in the Advanced Control Technology System in 1986, with responsibilities in the field of protection against environmental effects.

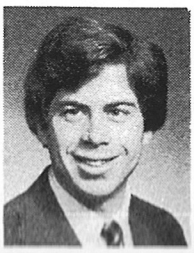

Joseph M. Pimbley (M'87–SM'91) received the B.S., M.S., and Ph.D. degrees in physics from the Rensselaer Polytechnic Institute, in Troy, NY, in 1980, 1981, and 1985, respectively. His doctoral research focused on the theoretical study of short-range atomic order at two-dimensional surfaces and overlayers. This thesis research received the H. B. Huntington Prize (Department of Physics) and the Karen and Lester Gerhardt Prize (School of Science).

After receiving the B.S. degree in 1980, he accepted a staff position in what is now the VLSI Technology Laboratory at the General Electric Corporate Research and Development Center, Schenectady, NY, and continued graduate study on a part-time basis. His interests at General Electric included the design and fabrication of visible and infrared solid-state image sensors and their performance in hostile radiation environments and the physics of high electric fields in semiconductor devices. He accepted the position of Assistant Professor in the Rensselaer Department of Mathematical Sciences in January 1987 where he studies semiconductor device issues and novel signal processing methods and teaches courses in applied mathematics, differential equations, proba-

bility theory and scientific computing. He received two Dushman awards for "outstanding technical contributions" during his General Electric years; he has published numerous technical papers in the fields of semiconductor device physics and surface atomic ordering and holds seven patents. He is the principal author of *Advanced CMOS Process Technology*, a research monograph published by Academic Press in 1989 as part of its series on VLSI Electronics.

Dr. Pimbley chairs the Annual Workshop on Applied Mathematics Problems in Industry at Rensselaer. He is a member of Sigma Pi Sigma, Sigma Xi, the IEEE Electron Devices Society, the Society of Industrial and Applied Mathematicians (SIAM), and the American Association for the Advancement of Science (AAAS).

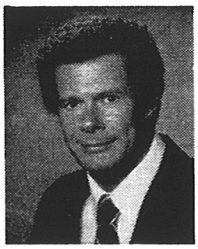

William E. Schneider received the B.S. degree in physics from Stetson University, De Land, FL, and the M.S. degree in metrology from George Washington University, Washington, DC.

He spent 7 years at the National Institute of Standards and Technology (NIST), Washington, DC, developing spectroradiometric standards, instrumentation, and measurement techniques. He is co-founder and President of Optronic Laboratories, Inc., Orlando, FL. He is the author or co-author of over 30 papers relating to the measurement of optical radiation.